

Original Research

## Structural Effectiveness of Fixed Offshore Platforms with Respect to Uniform Corrosion

Abubakar O. Salihu<sup>1</sup> , Kolawole Abejide<sup>2,\*</sup> , Olugbenga S. Abejide<sup>1</sup> , Jibrin M. Kaura<sup>1</sup> , Ibrahim Aliyu<sup>1</sup> , Kehinde Adeshina<sup>3</sup> , Olugbenga S. Abejide<sup>4</sup> 

<sup>1</sup> Department of Civil Engineering, Ahmadu Bello University, Zaria, Nigeria; salihuao@gmail.com (A.O. Salihu), osabejide@abu.edu.ng (O.S. Abejide), jmkaura@abu.edu.ng (J.M. Kaura), ibrahimaliyu@abu.edu.ng (I. Aliyu)

<sup>2</sup> Department of Civil Engineering, University of KwaZulu-Natal, Durban, South Africa

<sup>3</sup> Department of Construction Management, Ulster University, 2-24 York Street, Belfast, BT15 1AP, Northern Ireland, United Kingdom; Adeshinaolayinka03@gmail.com

<sup>4</sup> Council for Scientific and Industrial Research, Brummeria, Pretoria, South Africa; sabejide@csir.co.za

\* Correspondence: [koladeabejide@gmail.com](mailto:koladeabejide@gmail.com)

Received: 4 October 2024 / Accepted: 11 December 2024 / Published online: 30 December 2024

### Abstract

This study presents the structural effectiveness of fixed offshore platforms, addressing the challenges posed by complex loading conditions in marine environments. The structural performance of the fixed offshore platform was assessed using Finite Element Analysis performed in ABAQUS CAE software, with particular focus on the impact of intrinsic stress induced by corrosion and environmental loads such as; wind, waves, and operational activities. The reliability of the fixed offshore platform was also assessed using Monte Carlo's reliability method. The study utilized advanced design equations to evaluate the structural reliability and rate of corrosion of the fixed offshore platform in order to estimate the safety of the structure. Results indicated that there are high stress values in the beam and column connections and also in the columns due to the effect of depleting cross-sectional area with respect to time and also the intrinsic stresses as a result of the applied loadings. Hence, selecting a high-grade steel and a higher cross-sectional area for structural members will slow the rate of corrosion and also reduce the intrinsic stresses due to the loadings on the structure. This will not only improve the load-bearing capacity but also significantly reduced the risk of structural failure, aligning well with empirical data. Furthermore, the study highlighted the importance of considering the interaction between material properties, connection characteristics, and loading conditions in the design process. These findings contribute to the development of more robust and durable fixed offshore platforms, ensuring their safety and longevity in demanding operational environments.

**Keywords:** corrosion, finite element analysis, fixed-offshore platform, weld

## 1. Introduction

Fixed offshore platforms are vital structures in the energy sector, serving as essential hubs for extracting and processing oil and gas resources from beneath the ocean floor. The structural integrity of these platforms is of utmost importance, particularly given the severe and unpredictable marine environments in which they operate. The combination of harsh weather, corrosive saltwater, and dynamic loads presents significant challenges to the durability of these platforms. Steel beam and column joints, including welded connections, play a critical role in maintaining the platform's overall stability and load-bearing capacity, particularly when subjected to corrosion and fluctuating environmental forces (Abejide et al., 2022). Among the various structural elements, welded beam and column joints are integral to the platform's resilience, ensuring the transfer of loads between different components. These joints must withstand a combination of static and dynamic forces, including the weight of the platform, environmental loads from waves, wind, and ocean currents, as well as operational forces during drilling and production activities. The effects of corrosion further complicate this, as it reduces



the cross-sectional area of steel components, leading to reduced strength and increased vulnerability over time (He et al., 2023). As a result, ensuring the reliability of these joints is paramount for the long-term safety and operational efficiency of offshore platforms. Corrosion is particularly insidious in offshore environments, as the constant exposure to saltwater accelerates the deterioration of steel. In welded steel joints, corrosion can be even more problematic due to the presence of residual stresses from welding, which can act as initiation sites for cracks and corrosion pits. The presence of pitting corrosion, a localized form of corrosion, can drastically reduce the shear strength of welded joints, jeopardizing the platform's ability to withstand lateral forces and potentially leading to structural failure (Walter et al., 2024). Traditional design codes, such as SANS 10162 and AASHTO LRFD, offer general guidelines for designing welded joints and beams in offshore platforms, incorporating conservative safety factors to account for uncertainties. However, these codes may not fully account for the unique conditions encountered in marine environments, including corrosion degradation and complex load interactions. This highlights the growing need for more refined design methods that consider the specific challenges of offshore structures, especially under long-term exposure to corrosive conditions (Brijder et al., 2022). Recent advancements in computational modeling, such as Finite Element Analysis (FEA), have transformed the study of welded joints under complex loading and corrosion conditions. FEA allows for detailed simulations of stress distributions, deformation patterns, and potential failure modes in steel joints, considering the effects of corrosion on material properties and structural behavior. By integrating corrosion models into FEA, engineers can predict how corrosion-induced material loss affects the long-term reliability of the structure. This, in turn, provides insights into the development of mitigation strategies, such as optimized weld geometries, improved material selection, and protective coatings that enhance corrosion resistance (Zhou et al., 2024). Moreover, reliability analysis plays a crucial role in understanding the performance of offshore platforms over their service life. Reliability-based design approaches allow engineers to quantify the probability of failure and assess the long-term durability of welded joints subjected to corrosion. This is essential in ensuring that offshore platforms maintain a high level of safety and functionality despite the inevitable degradation of materials. Reliability modeling also helps in determining maintenance intervals and predicting when structural interventions may be needed, reducing the risk of catastrophic failures in service (Ghanadi et al., 2024).

This study seeks to address the critical issues of corrosion, shear strength, and reliability in welded steel beam and column joints in offshore platforms. By employing a combination of experimental investigations, numerical simulations, and reliability-based assessments, the research aims to develop practical design recommendations that improve the durability, safety, and cost-effectiveness of offshore structures. Understanding the behavior of welded joints under real-world conditions, including the impact of corrosion, is key to enhancing the resilience of offshore energy infrastructure for years to come.

## 2. Background of study

### 2.1. Welded column behavior in offshore environments

Welded steel columns are fundamental components in offshore platforms due to their capacity to bear axial and lateral forces. These columns in offshore structures endure complex loading conditions, including wave, wind, and seismic forces. A significant concern in such environments is the combination of these loads with the corrosive effects of seawater, which degrades the material over time, particularly at the welds. Weld quality is critical, as defects in welds substantially reduce the shear strength and overall stability of the columns (Wang et al., 2024a). The shear strength of a welded steel column can be estimated using classical shear strength theory. For thin-walled structures like I-section or tubular columns, which are common in offshore applications, the shear strength  $V$  is given by:

$$V = A_w \cdot \tau_{max} \quad (1)$$

where  $A_w$  is effective shear area of the web and  $\tau_{max}$  is maximum shear stresses the material can withstand.

In welded connections, the properties of the weld metal and its geometry significantly influence  $\tau_{max}$ . The welding process induces residual stresses and alters the microstructure at the heat-affected zone (HAZ), creating stress concentration points that reduce the effective shear strength (Rautiainen et al., 2023). Researches emphasize that corrosion-induced deterioration in the weld zone reduces the

ultimate shear capacity of welded joints in offshore platforms. Their study showed a decrease of up to 25% in shear strength within the first five years of seawater exposure (Wang et al., 2024b). Methods like applying corrosion-resistant coatings and performing post-weld heat treatments can improve the longevity and shear strength of these columns.

## 2.2. Shear strength optimization using welding techniques and codes

Optimizing the shear strength of welded columns involves careful material selection, advanced welding techniques, and strict adherence to design codes such as AWS D1.1: Structural Welding Code – Steel (American Welding Society, 2020) and ISO 19902 standard (International Organization for Standardization, 2020a). These codes specify the required weld size, material grade, and prequalification criteria for offshore applications, where extreme environmental conditions necessitate stronger and more reliable welded joints.

The AWS D1.1 structural welding code (American Welding Society, 2020) specifies that the design shear strength of a welded steel column  $V_n$  is calculated as:

$$V_n = 0.6 \cdot F_y \cdot A_w \quad (2)$$

where  $F_y$  is yield strength of the steel material,  $A_w$  is effective shear area.

For offshore platforms, this equation is adjusted to account for dynamic loading conditions like wave action and wind forces by introducing a dynamic load factor  $\gamma_d$ :

$$V_n = 0.6 \cdot F_y \cdot A_w \cdot \gamma_d \quad (3)$$

Welding techniques such as Submerged Arc Welding (SAW) and Friction Stir Welding (FSW) have been extensively researched for their ability to produce high-quality welds with minimal (Kollár, 2023). Friction Stir Welding, in particular, offers significant advantages by reducing common defects such as porosity and cracking, which adversely affect shear strength in the welded zone. The resulting joints exhibit higher fatigue resistance and lower stress concentrations, enhancing shear performance under cyclic loading conditions (Dutta et al., 2024). Research demonstrated that FSW increases the shear strength of welded offshore columns by 18% compared to traditional Gas Metal Arc Welding (GMAW). This improvement is attributed to the uniform microstructure and reduced residual stresses, leading to higher effective shear strength in both the weld zone and the surrounding material (Chen et al., 2024b).

## 2.3. Structural welding

Structural welding is a process by which the parts that are to be connected are heated and fused with supplementary molten metal at the joint. A relatively small depth of material will become molten, and upon cooling, the structural steel and weld metal will act as one continuous part where they are joined (Chen et al., 2024a).

Fillet welds are most common and used in all structures. Weld sizes are specified in 1/16 in. (1.5875 mm) increments. A fillet weld can be loaded in any direction in shear, compression, or tension. However, it always fails in shear (Şeker, 2021). In the simulations, E70XX welding electrodes were selected due to their compatibility with the base metal (S460 high strength structural steel). These electrodes have a tensile strength of 482 N/mm<sup>2</sup>, which closely matches the base material's yield strength of 460 N/mm<sup>2</sup>, ensuring minimal residual stresses and consistent mechanical properties in the welded zone. The chemical composition of the welding consumables was also chosen to align with that of the base steel, maintaining similar carbon equivalence and corrosion resistance. This ensures the mechanical and chemical homogeneity of the joint, which is critical for accurate finite element simulations and the reliability of offshore structures under corrosive conditions. The shear failure of the fillet weld occurs along a plane through the throat of the weld, as shown in the Fig. 1.

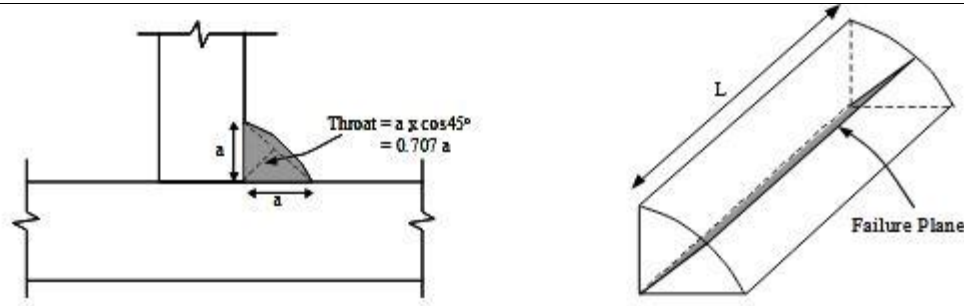


Fig. 1. Welded steel joint.

Table 1 shows the tensile strength of weld electrodes and their corresponding standard nomenclature.

Table 1. Tensile strength of weld electrodes (Pradhan et al., 2022)\*.

Nomenclature of corresponding electrode	Tensile strength of weld electrode (ksi)	Tensile Strength (N/mm <sup>2</sup> )
E60XX	60	$60 \times 6.89476 = 413.69$
E70XX	70	$70 \times 6.89476 = 482.63$
E80XX	80	$80 \times 6.89476 = 551.58$
E90XX	90	$90 \times 6.89476 = 620.53$
E100XX	100	$100 \times 6.89476 = 689.48$
E110XX	110	$110 \times 6.89476 = 758.42$
E120XX	120	$120 \times 6.89476 = 827.37$

\*Note: The strength of the electrode should match the strength of the base metal.

## 2.4. Monte Carlo reliability method

Monte Carlo simulations play a vital role in assessing the reliability of steel structures in offshore environments due to the inherent uncertainty in material properties, loadings, and environmental conditions. Offshore steel structures, such as platforms, are subjected to various corrosive forces that lead to the degradation of structural integrity over time, significantly affecting their reliability (Elqars et al., 2024). In the context of reliability analysis, Monte Carlo methods allow engineers to model these uncertainties by simulating numerous potential outcomes and quantifying the probability of failure ( $P_f$ ) and the reliability index ( $\beta$ ).

$$\beta = \frac{\mu_R - \mu_S}{\sqrt{\sigma_R^2 + \sigma_S^2}} \quad (4)$$

where  $\mu_R$  and  $\sigma_R$  are the mean and standard deviation of the resistance,  $\mu_S$  and  $\sigma_S$  are the mean and standard deviation of the loading

$$P_f = \int_{-\infty}^0 f_g(g) dg \quad (5)$$

where  $f_g(g)$  is the probability density function of the limit state function  $g(x)$ .

The limit state function for the fixed offshore platform is given by:

$$P_f = \int_{-\infty}^0 f_g(g) dg \quad (6)$$

where  $A_0$  is Initial cross-sectional area of the structural member;  $\Delta A(t)$  is the cross-sectional area loss due to corrosion as a function of time  $t$ ;  $f_y$  is the yield strength of the steel;  $S_{wave}$ ,  $S_{wind}$ ,  $S_{current}$  are forces from waves, wind, and currents, respectively

Failure occurs when  $g(x) \leq 0$ , meaning that the applied loads exceed the structure's resistance.

## 3. Methodology

The offshore structure was subjected to high axial and lateral loads due to design loading and environmental conditions such as waves, wind, and current. In this analysis a fixed offshore platform is modeled, and loaded with respect to the design load as per AASHTO LRFD (American Association of State Highway and Transportation Officials, 2020) and ISO 19902:2020 (International Organization for Standardization, 2020a). The beam and column sections used are UB 254×102×25 and UB

356×137×33 respectively. These sections are fabricated using the hot-rolling process, which results in more uniform mechanical properties compared to cold-rolled or welded sections. Hot-rolled sections were selected for their superior performance in resisting dynamic loads and their higher reliability in corrosive environments. AWS D1.1/D1.1M (American Welding Society, 2020) is used to design the weld connection between the beam and column sections (American Institute of Steel Construction, 2024). The effect of uniform corrosion is also considered on the offshore structure over a design period of 50 years under service conditions. The intrinsic stress due to the applied loading and corrosion is then analyzed. The reliability of the structure during the course of its service life was also evaluated using Monte Carlo's reliability method.

### 3.1. Standard expression for corrosion rate

The fixed offshore platform is also being affected by uniform corrosion during its service life. This will lead to cross sectional area loss and more induced stress as the cross section available for carrying load is depleted (Soufnay et al., 2024). The formula for calculating corrosion rate ( $CR$ ) is

$$CR = \frac{mm}{years} = 87.6 \frac{W}{DAT} \quad (7)$$

where  $W$  is weight loss in milligrams,  $D$  is density in  $g/mm^3$ ,  $A$  is area in  $mm^2$  and  $T$  is time of exposure in hours.

### 3.2. Steel cross sectional area loss

Cross-sectional area loss in steel structures, especially offshore platforms, is primarily caused by corrosion. Over time, exposure to harsh marine environments leads to the degradation of steel, reducing the effective cross-sectional area of critical structural components (Soufnay et al., 2024). This reduction increases the stress concentration on the remaining material, thereby weakening the structure and raising the probability of failure.

$$A(t) = A_0 \left(1 - \frac{CR \cdot t}{100}\right) \quad (8)$$

where  $A_0$  is the initial cross-sectional area,  $CR$  is the corrosion rate (% loss per year) and  $t$  is the time in years

### 3.3. Load analysis

Several live load components are included in the AASHTO LRFD (American Association of State Highway and Transportation Officials, 2020) and ISO 19901-3:2020 (International Organization for Standardization, 2020b). Specifications, which were combined and scaled to provide design live loads. Included among the elements are: The AASHTO LRFD design specifications and ISO 1991-3:2020), which are a widely used design code for offshore structures in countries across the globe.

#### 3.3.1. Offshore platform live load

The fixed platform live load consists of four components (International Organization for Standardization, 2020b):

- Personnel loads = 2 kN/m<sup>2</sup>
- Equipment loads = 5 kN/m<sup>2</sup>
- Storage loads = 7 kN/m<sup>2</sup>
- Dynamic loads = 5 kN/m<sup>2</sup>

Live load acting on the fixed platform = 2 + 5 + 7 + 5 = 19 kN/m<sup>2</sup>

These four components; the personnel loads, equipment loads, storage loads, dynamic loads, are combined to create the model for live load

#### 3.3.2. Offshore platform dead load

Dead load consists of three components (International Organization for Standardization, 2020b):

- Permanent equipment dead load = 5 kN/m<sup>2</sup>
- Structural steel dead load = 10 kN/m<sup>2</sup>
- Sacrificial anode (aluminum alloy) dead load: **5 kN/m<sup>2</sup>**



Total sum of dead load (estimated) =  $5 + 10 + 5 = 20 \text{ kN/m}^2$

Taking into consideration: environmental loads, construction loads, and so on, the dead load will be approximated =  $25 \text{ kN/m}^2$

The AASHTO LRFD Design Specification (3.4.1 – Load factors), for factored loading design load can be determined from the relationship ([American Association of State Highway and Transportation Officials, 2020](#)):

$$\text{Design load} = 1.25\mathbf{D} + 1.75\mathbf{L} \quad (9)$$

where  $\mathbf{D}$  represents the dead load and  $\mathbf{L}$  represents the live load.

The load factors of 1.2 and 1.6 are specific to the AASHTO LRFD code and may vary in other LRFD design codes. Therefore:

$$\text{Design load} = 1.25[25] + 1.75[19] = 31.25 + 33.25 = 64.50 \text{ kN/m}^2$$

### 3.4. Offshore platform design according to AASHTO LRFD 2020

The offshore platform model was analyzed as a fixed platform, meaning its base was fully constrained to simulate real-world conditions where the foundation is anchored to the seabed. The boundary conditions applied include fixing all degrees of freedom (translations and rotations) at the base to replicate this support. Fig. 2 illustrates the boundary conditions applied to the platform model. These conditions were essential for accurately modeling the platform's response to environmental loads and the design load.

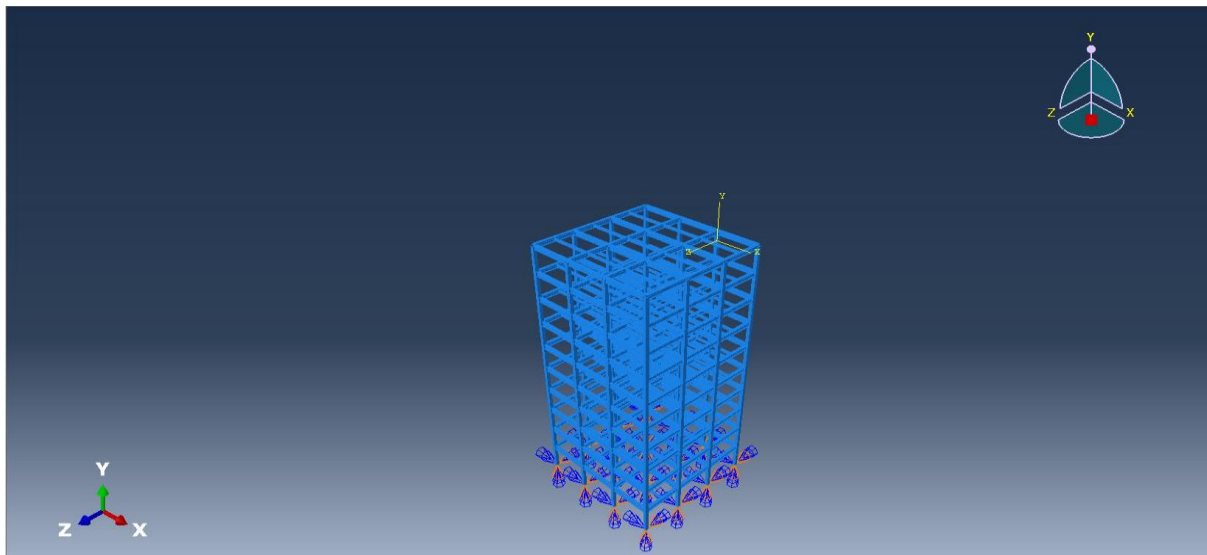


Fig. 2. Boundary condition of the fixed offshore platform (Encastre).

Table 2 gives the essential design parameters for the stochastic analysis used in the probabilistic determination of the safety criteria of the steel material.

Table 2. Parameters of stochastic model.

Material	Density	Young's modulus	Yield Stress	Poisson's ratio $\nu$	Strain
Steel	$7850 \text{ kg/m}^3$	210 GPa	$460 \text{ N/mm}^2$	0.3	0.0022

Fig. 3a illustrates the cross-sectional dimensions of the UB 254×102×25 beam, which was selected for the analysis of the fixed offshore platform. These dimensions provide the baseline reference for evaluating the structural performance of the beam under design and environmental loads. The beam's cross-section was integral to the FEA conducted in ABAQUS, where its geometric properties influenced stress distribution, deformation, and resistance to uniform corrosion.

Fig. 3b depicts the cross-sectional dimensions of the UB 356×137×33 column, used as a key structural element in the fixed offshore platform analysis. The column's geometry and size were critical in determining its load-bearing capacity, particularly under combined axial and lateral forces. This reference drawing serves as the foundation for incorporating the column into the FEA model, where its dimensions affected stress concentrations and reliability outcomes.

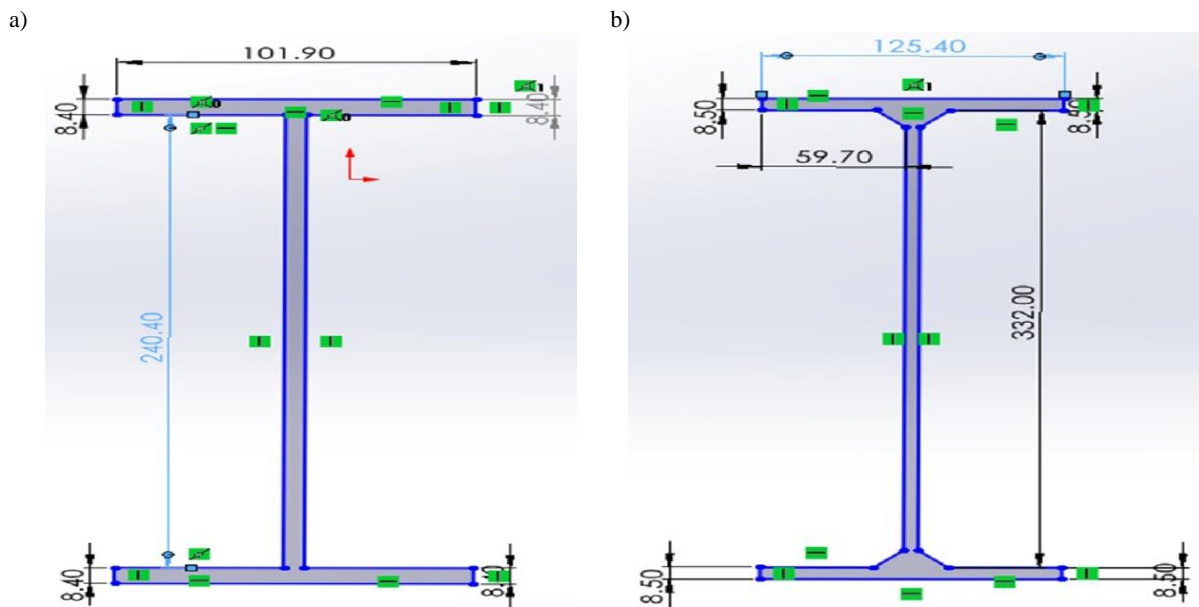


Fig. 3. a) steel beam cross section (UB 254×102×25) and b) steel column cross section (UB 356×137×33).

## 4. Results and discussion

### 4.1. Finite element analysis in Simulia ABAQUS CAE 2022

The fixed offshore platform was analyzed using Simulia ABAQUS CAE 2022 with respect to AASHTO-LRFD (American Association of State Highway and Transportation Officials, 2020) and AWS D1.1/D1.1M (American Welding Society, 2020). ABAQUS CAE does analysis based on finite element method and the analysis completed for this research is with respect to uniform corrosion in offshore and the effect on the integrity of the offshore structure. Over the course of 100 years at an interval of 10 years, the reduction in cross-sectional area with respect to uniform corrosion was examined in order to check the intrinsic stresses induced while in service. The reliability and the probability of failure of the fixed offshore structure was also evaluated using Monte Carlo's reliability method. The fixed offshore platform was subjected to design load of 64.50 kN/m<sup>2</sup>. The FEA of the fixed platform following a non-linear stress pattern are also discussed below.

#### 4.1.1. Von Mises stress distributions over fixed offshore platform in service condition

The fixed offshore platform subjected to uniform corrosion over a 100-year period exhibited increasing von Mises stresses due to cross-sectional area loss and material degradation. A non-linear finite element analysis revealed that after 10 years, maximum von Mises stresses were 7.846 N/mm<sup>2</sup>, as shown in Fig. 4. By 50 years, these values increased to 8.000 N/mm<sup>2</sup> as shown in Fig. 5. After 100 years, the stresses reached 8.311 N/mm<sup>2</sup> as shown in Fig. 6. These findings confirm that uniform corrosion significantly affects the structural integrity of the platform over time, particularly at the columns and joints due to load transfer mechanisms. The von Mises stress criterion used here indicates the platform's susceptibility to yielding and potential failure. Importantly, despite the increase in stresses, the results remain within acceptable limits  $\frac{f_y}{1.5}$  for S460 high strength structural steel. According to EN 10025-4:2023 (European Committee for Standardization, 2023), the yield strength of S460 grade steel is  $f_y = 460$  N/mm<sup>2</sup> and its ultimate tensile strength ranges from 550 to 720 N/mm<sup>2</sup>. The design stresses computed in this analysis do not exceed  $f_y$  when factoring in partial safety factors as per AASHTO LRFD (American Association of State Highway and Transportation Officials, 2020). The progressive stress accumulation highlights the detrimental impact of cross-sectional depletion, emphasizing the need for preventive measures to slow corrosion and maintain the platform's structural capacity.

The results underscore that while the platform's integrity remains intact within the design parameters, continued corrosion would necessitate reinforcement strategies and regular maintenance. This study demonstrates that addressing corrosion early could prolong the platform's lifespan and maintain its operational safety.

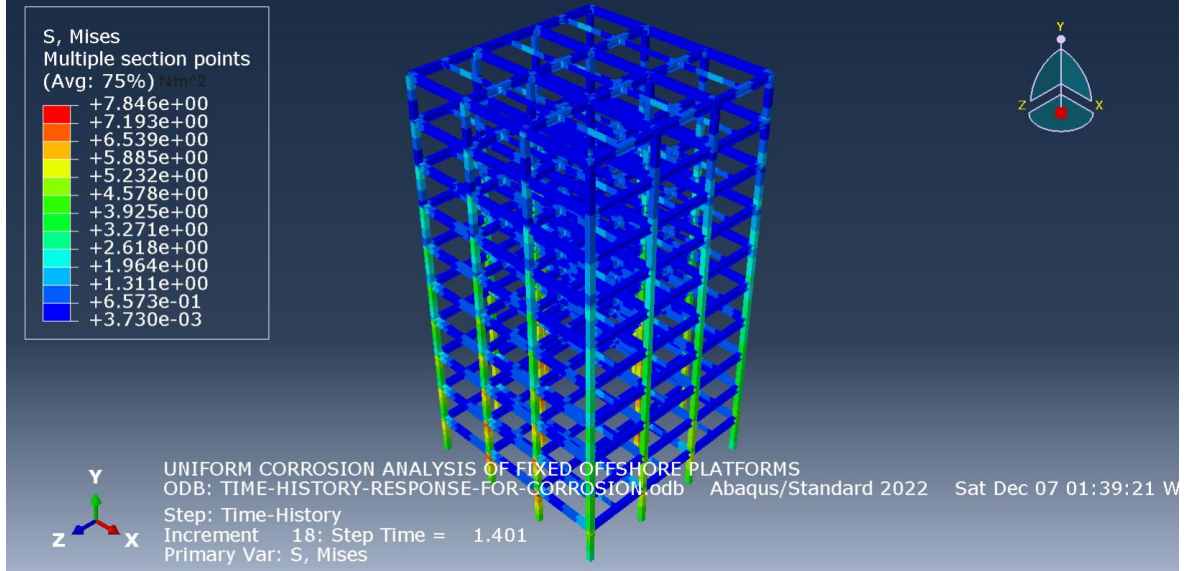


Fig. 4. Von Mises stress distribution (in  $N/m^2$ ) of the fixed offshore platform with respect to corrosion at 10 years.

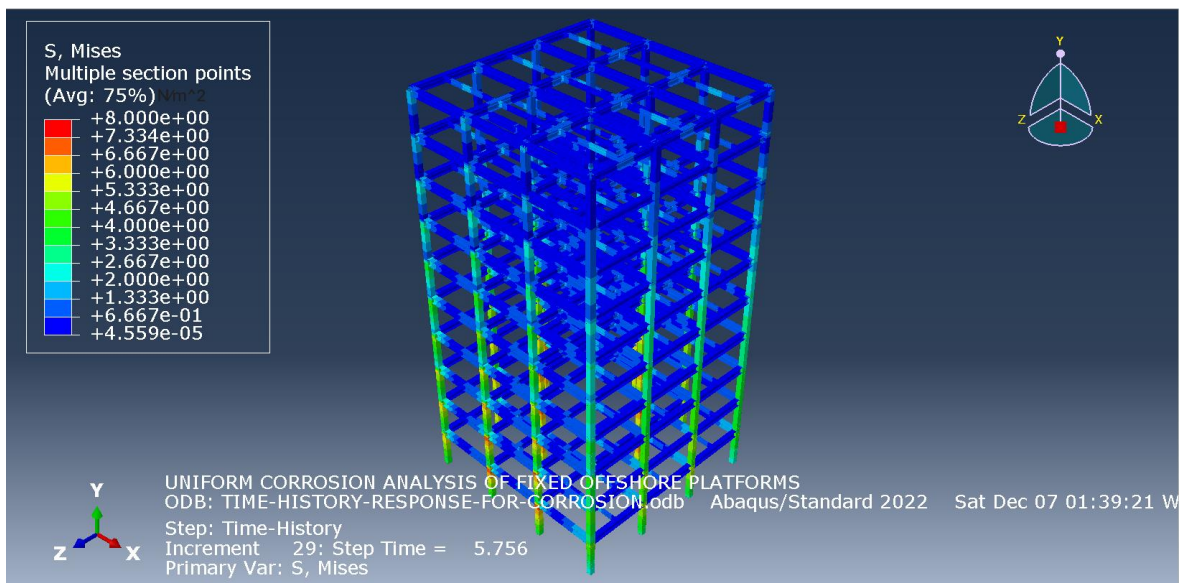


Fig. 5. Von Mises stress distribution (in  $N/m^2$ ) of the fixed offshore platform with respect to corrosion at 50 years.

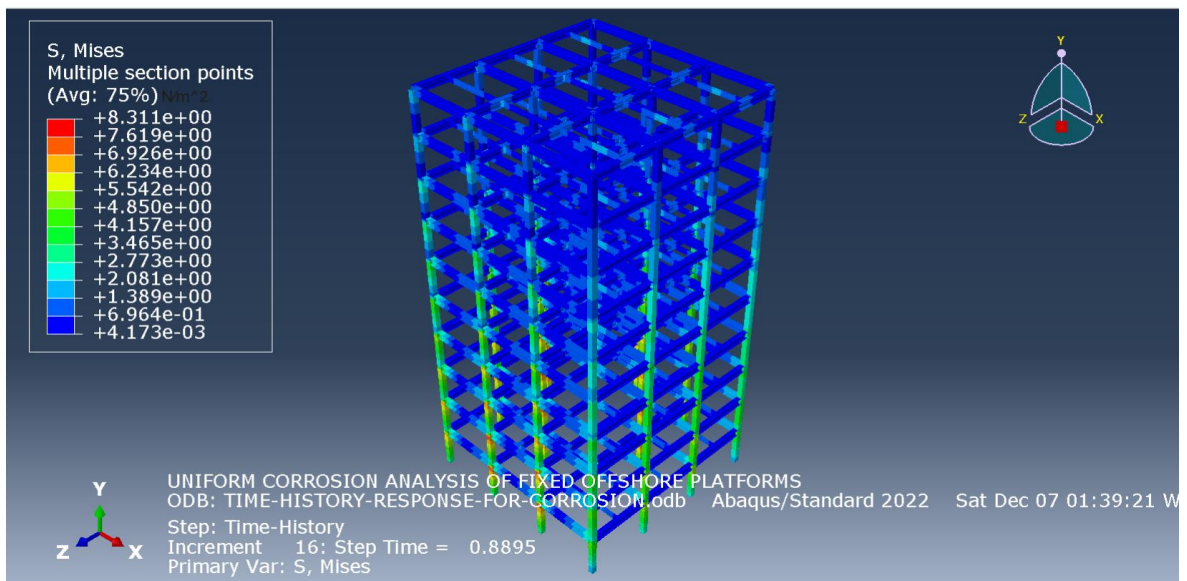
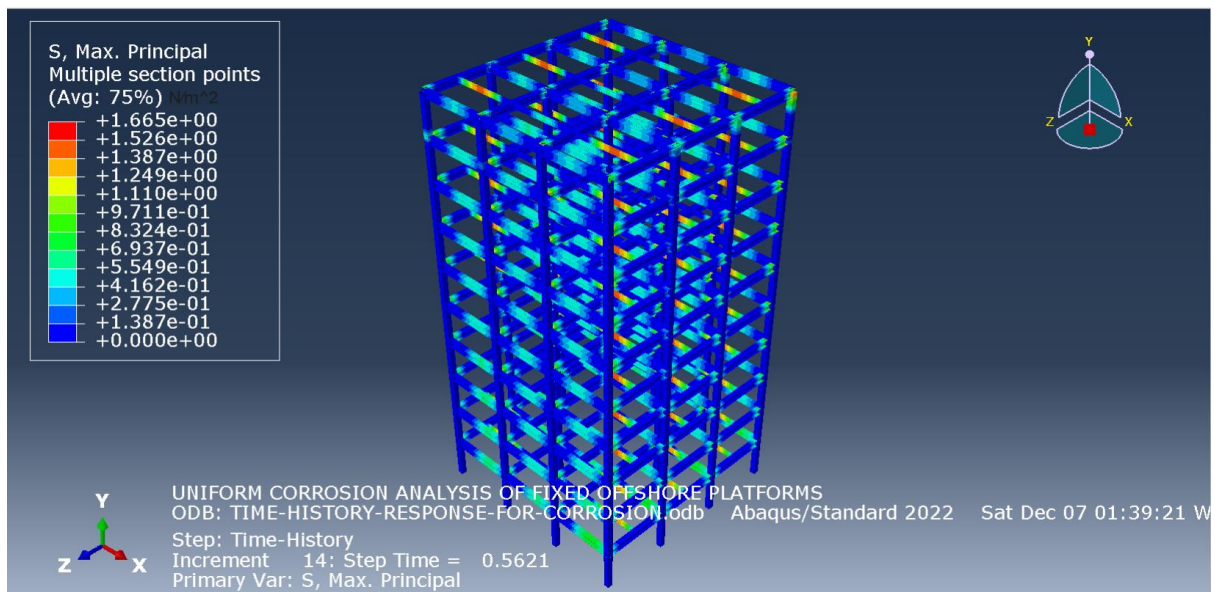


Fig. 6. Von Mises stress distribution (in  $N/m^2$ ) of the fixed offshore platform with respect to corrosion at 100 years.



#### 4.1.2. Maximum principal stress distributions over fixed offshore platform in service condition

The fixed offshore platform under service conditions experienced increasing maximum principal stresses due to uniform corrosion and service loading. After 10 years, the maximum principal stress reached 1.665 N/m<sup>2</sup> as shown in Fig. 7, primarily concentrated at the columns and joints due to load transfer mechanisms. This trend intensified, with stress values rising to 1.940 N/m<sup>2</sup> as shown in Fig. 8 after 50 years and 2.253 N/m<sup>2</sup> as shown in Fig. 9 after 100 years. The progressive increase in maximum principal stresses highlights the critical impact of uniform corrosion on the platform's structural integrity. Although the stresses remain within the allowable limits  $0.66\sqrt{f_{yk}}$ , the rising trend indicates an elevated risk of localized failure over time, especially in areas subjected to high stress concentrations. These findings underscore the need for proactive maintenance strategies, including regular inspections and corrosion protection measures, to mitigate long-term degradation. The maximum principal stress distributions reveal that the platform's structural health degrades with time due to corrosion, emphasizing the importance of continuous monitoring to ensure safe operation over its service life.



**Fig. 7.** Maximum principal stress distribution (in N/m<sup>2</sup>) of the fixed offshore platform with respect to corrosion at 10 years.

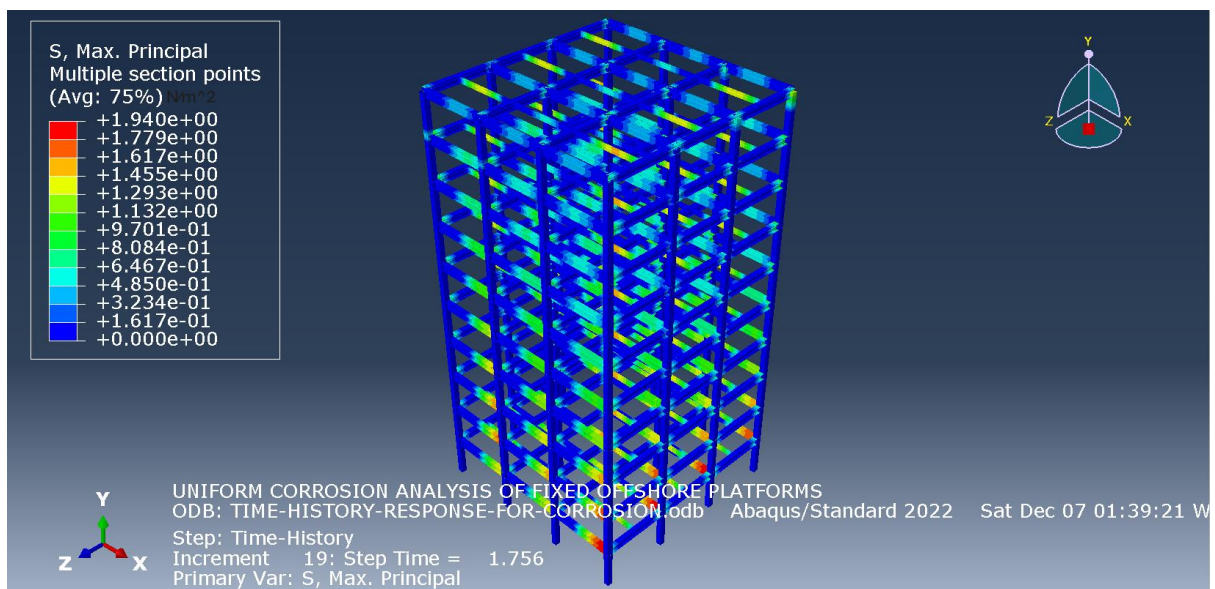


**Fig. 8.** Maximum principal stress distribution (in N/m<sup>2</sup>) of the fixed offshore platform with respect to corrosion at 50 years.

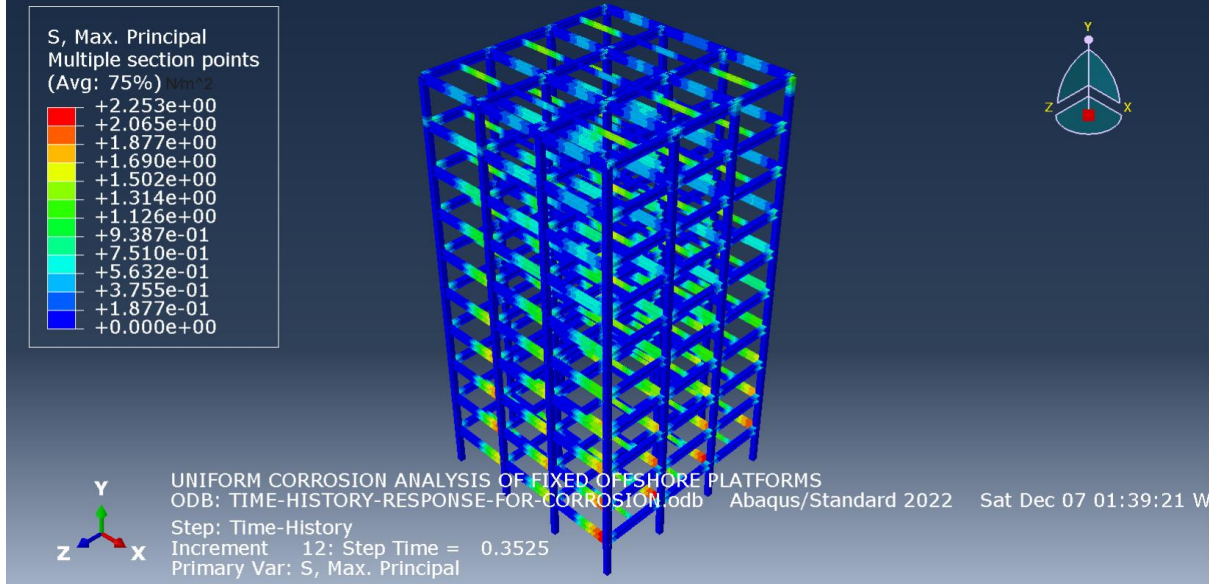


**Fig. 9.** Maximum principal stress distribution (in N/m<sup>2</sup>) of the fixed offshore platform with respect to corrosion at 100 years.

4.1.3. Tresca stress distributions over fixed offshore platform in service condition

The Tresca stress distribution in the fixed offshore platform subjected to uniform corrosion and design loading conditions reveals critical insights into its structural performance. At 10 years, the maximum Tresca stress reached 7.850 N/m<sup>2</sup> as shown in Fig. 10, with significant concentrations at the column bases and joints. By 50 years, the maximum stress increased to 8.000 N/m<sup>2</sup> as shown in Fig. 11, primarily due to cross-sectional area loss from corrosion, leading to higher stress concentrations around connections. After 100 years, the maximum Tresca stress reached 8.311 N/m<sup>2</sup> as shown in Fig. 12, indicating the potential for yielding and plastic deformation in highly stressed regions. The increasing shear stress over time highlights the platform's decreasing capacity to resist failure, particularly in areas subjected to load transfer. The progression of Tresca stress, driven by corrosion, suggests that beyond 50 years, the structure approaches critical stress levels, requiring maintenance or reinforcement to prevent yielding. The analysis confirms that while the platform remains within safe operating limits in the early years, the continuous rise in Tresca stress underlines the need for timely intervention to ensure long-term structural integrity.

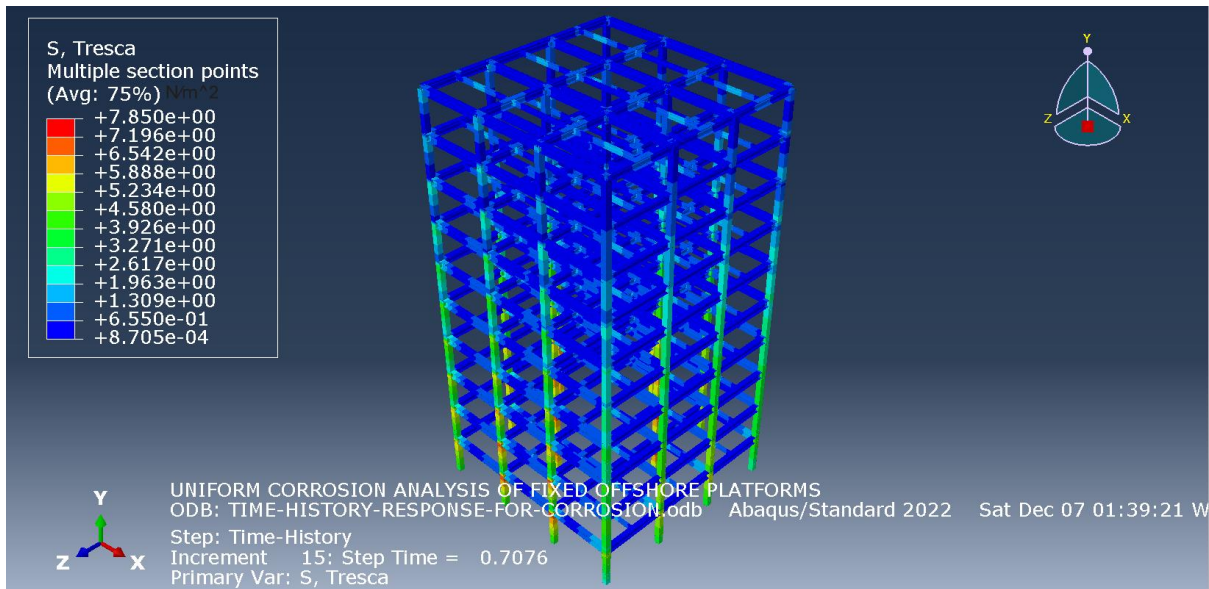


**Fig. 10.** Tresca stress distribution (in N/m<sup>2</sup>) of the fixed offshore platform with respect to corrosion at 10 years.



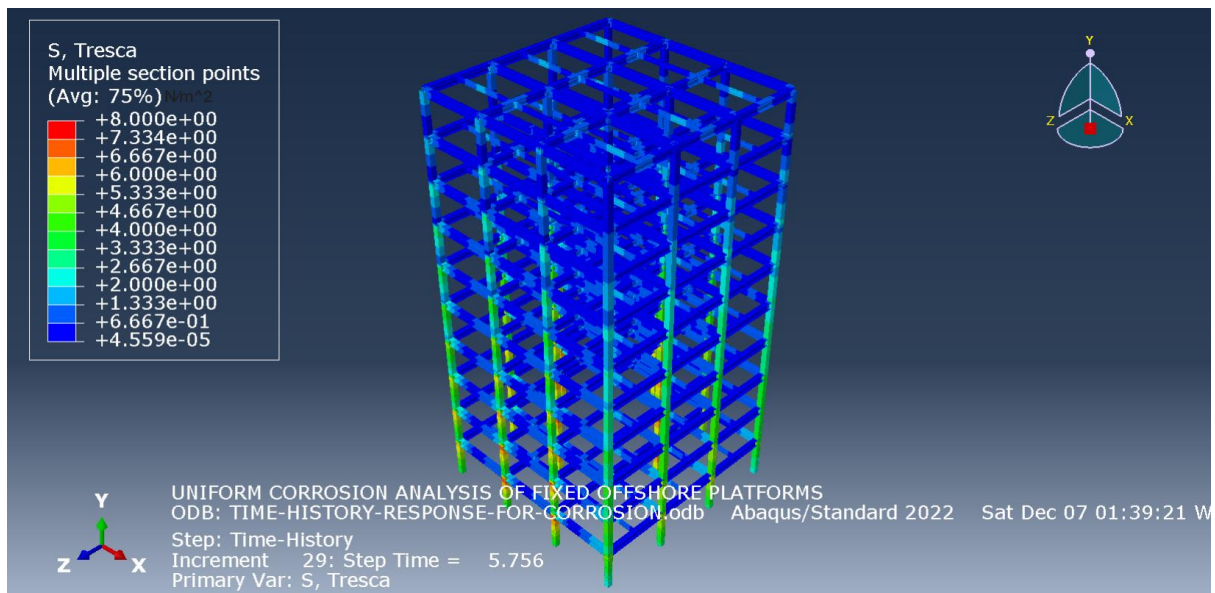


Fig. 11. Tresca stress distribution (in  $N/m^2$ ) of the fixed offshore platform with respect to corrosion at 50 years.

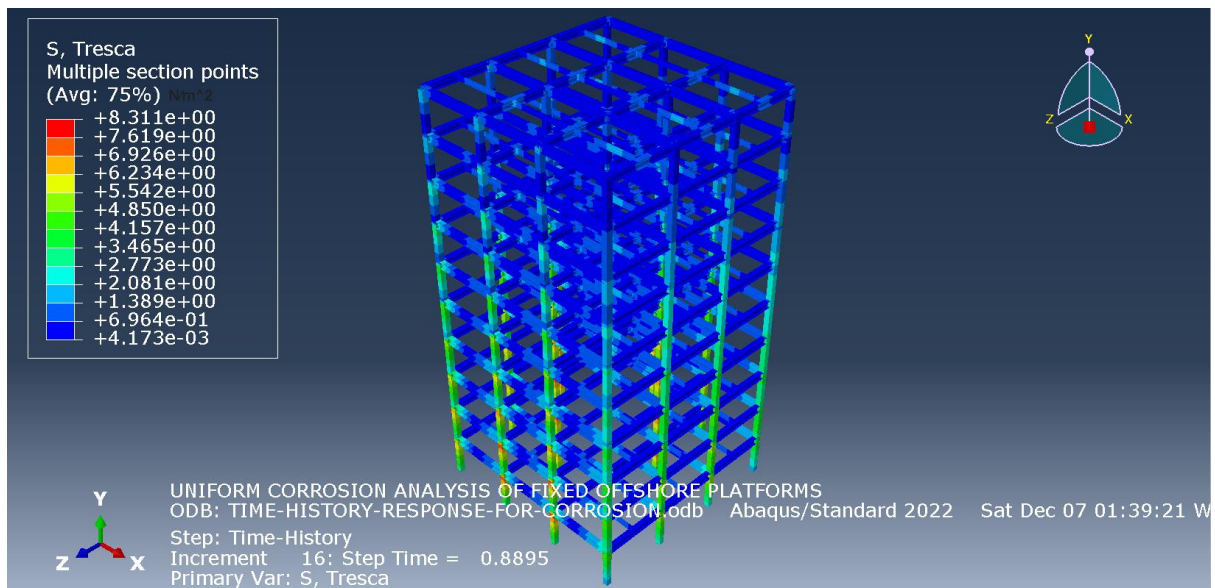


Fig. 12. Tresca stress distribution (in  $N/m^2$ ) of the fixed offshore platform with respect to corrosion at 100 years.

Table 3 below captures the maximum stress distributions with respect to uniform corrosion over the course of the design period of the fixed offshore platform from the FEA in Simulia ABAQUS 2022 software.

Table 3. Maximum stress distributions in the fixed offshore platform during its service period.

Stress ( $N/m^2$ )	Period		
	10 Years	50 Years	100 Years
von Mises	7.846	8.000	8.311
maximum principal	1.665	1.940	2.253
Tresca	7.850	8.000	8.311

Fig. 13 shows a graphical representation of the FEA stress distribution over the fixed offshore platform. The values of the von Mises stress distribution and the Tresca stress distribution are closely similar hence the lines lap each other in the plot. Since von Mises stress is similar to the Tresca stress in the analysis of a fixed offshore platform, it implies that the material is experiencing uniform or nearly uniform stress conditions, particularly shear stress. This indicates that the principal stresses are distributed in a way that yields minimal differences between the distortion energy theory (von Mises) and maximum shear stress theory (Tresca). Such similarity suggests the structure is well-designed to handle the applied loading, with predictable material behavior and reduced complexity in evaluating

safety factors. This alignment highlights the platform's structural efficiency and durability under its operational conditions.

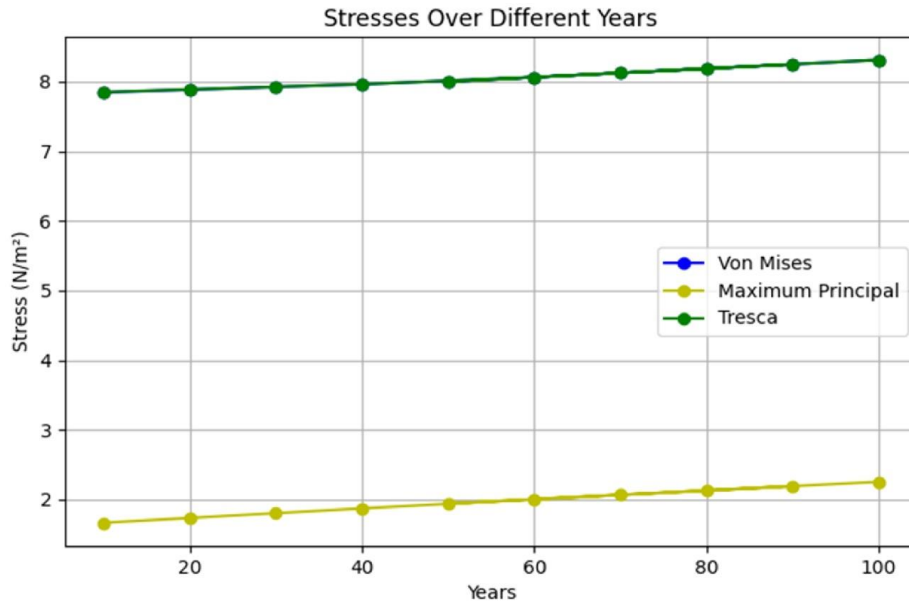


Fig. 13. Graphical representation of the stress distributions in the fixed offshore platform during its service life.

#### 4.2. Monte Carlo's reliability analysis in PYTHON

This section discusses the findings of the reliability analysis using the Monte Carlo reliability analyses method conducted on the fixed offshore structure using an algorithm in PYTHON to examine and simulate the behavior of the fixed offshore platform on exposure to uniform corrosion during a design period of 100 years. Through an interval of 10 years, the reduction in cross-sectional area, the probability of failure, and the reliability of the structure was examined using the expression for the rate of corrosion and the limit state equation in order to check the structural effectiveness of the fixed offshore structure while in service, resisting the effect of moment, deflection and shear. Monte Carlo's reliability method coded in PYTHON is employed in the computation, making use of the tabulated data in Table 4 and the relevant limit state functions and the rate of corrosion expression.

Table 4. Parameters of the stochastic model for rolled steel beams on offshore platforms.

S/No	Design Variables	Unit	Distribution Type	COV	E(Xi)	S(Xi)
1	Steel strength ( $f_{yk}$ )	N/mm <sup>2</sup>	Lognormal	0.15	350	52.5
2	Length (L)	mm	Normal	0.045	9000	450
3	Width (W)	mm	Normal	0.045	9000	450
4	Depth (d)	mm	Normal	0.15	30000	1500
5	Area of the structure	mm <sup>2</sup>	Normal	0.3	$8.1 \times 10^7$	$2.43 \times 10^6$
6	Imposed load $Q_k$	kN/m <sup>2</sup>	Lognormal	0.3	$5.0 \times 10^{-3}$	$1.5 \times 10^{-3}$
7	Wind load ( $W_k$ )	kN/m <sup>2</sup>	Lognormal	0.3	$5.0 \times 10^{-3}$	$1.5 \times 10^{-3}$
8	Wave load ( $W_p$ )	kN/m <sup>2</sup>	Lognormal	0.25	$7.0 \times 10^{-3}$	$2.1 \times 10^{-3}$
9	Current load ( $C_k$ )	kN/m <sup>2</sup>	Lognormal	0.25	$3.0 \times 10^{-3}$	$0.9 \times 10^{-3}$

The reliability levels were calculated using the deterministic and statistical parameters of Table 4. The *Coefficient of Variation* (COV) highlights the relative uncertainty of each parameter, identifying which variables are more prone to variability and impact reliability. The *Expected Value* (E(Xi)) represents the average performance or baseline value of each parameter, serving as the foundation for structural analysis. The *Standard Deviation* (S(Xi)) measures the dispersion of each parameter, indicating the range of possible deviations from the mean that influence design consistency and reliability. The rate of corrosion equation and the limit state equation  $g(x)$  was used based on Monte Carlo's reliability method in a PYTHON algorithm. The Fig. 14 depict the cross-sectional area loss of the fixed offshore structure with respect to time during its service period, the reliability of the fixed offshore structure with respect to time during its service period, and also the probability of failure of the fixed platform during its service period.

Based on the plot for the *Cross-Sectional Area Loss Over Time*, there is a steady linear increase in cross-sectional area loss for both the UB 254×102 beam (blue) and UB 356×137 column (green). As the years progress, corrosion causes the cross-sectional areas of both components to degrade, with the



column experiencing slightly higher losses due to its larger size. This reflects the expected cumulative material degradation from corrosion.

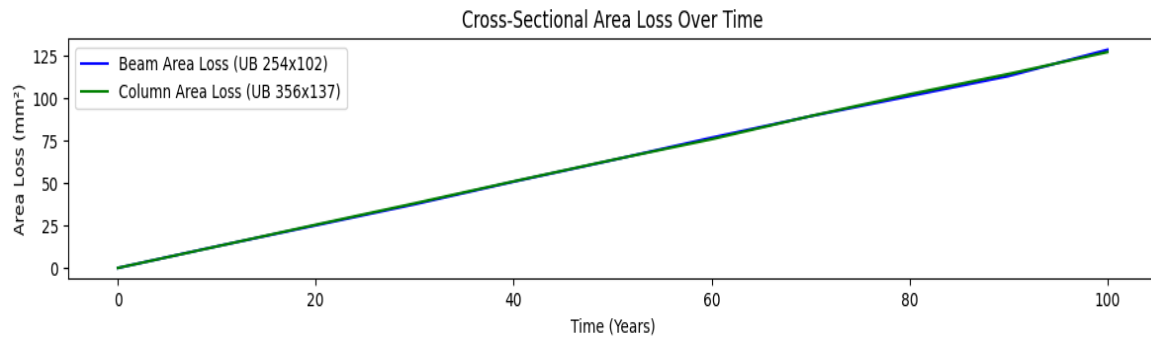


**Fig. 14.** A plot showing the relationship between corrosion in years and cross-sectional area loss of structural steel during its service life.

Based on the plot for the *Reliability Over Time* (Fig. 15), there is a progressive decrease in reliability over time for the UB 254×102 beam (blue) and the UB 356×137 column (green). The beam shows a more significant decline in reliability, suggesting it is more sensitive to cross-sectional area loss due to its size. This curve reflects the structural system's weakening due to material degradation, leading to lower reliability as time progresses. The cross-sectional area of is directly proportional to the reliability of the structure. Hence, a larger cross-sectional area implies a slower area loss.

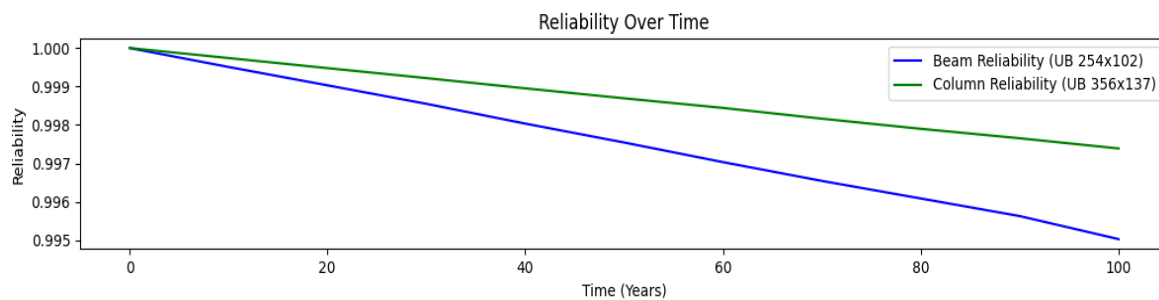


**Fig. 15.** A plot showing the relationship between reliability of the fixed offshore platform during its service life during its service life.

Based on the plot for *Probability of Failure Over Time* (Fig. 16) for the fixed offshore platform in service, there is an increasing probability of failure over time as the structure becomes more vulnerable due to corrosion. The UB 254×102 beam's probability of failure (red) grows more rapidly than the UB 356×137 column's (orange), indicating that the beam is more likely to fail sooner due to its smaller initial cross-sectional area. This implies that a smaller cross-sectional area is more susceptible to failure than a larger cross-sectional area as corrosion is simply the degradation and area loss of steel.

Corrosion has a progressive impact on the integrity of the structural steel in the fixed offshore structure making it vulnerable in terms of its reliability and it increases failure probability.

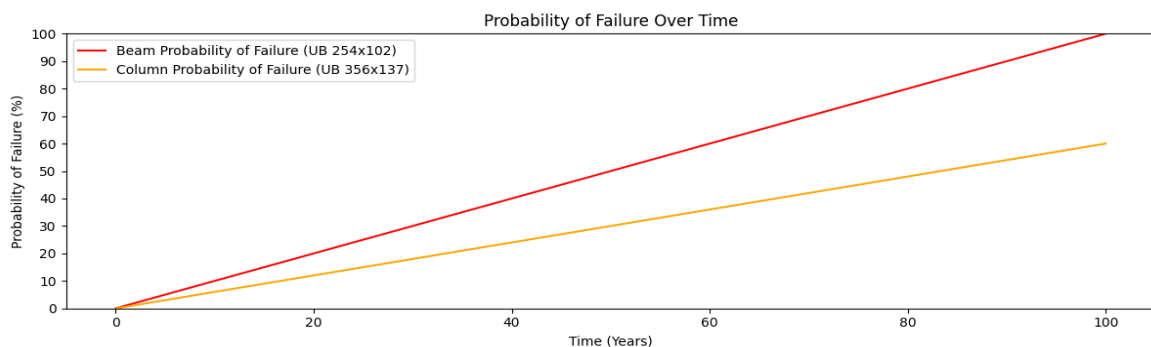


**Fig. 16.** A plot showing the relationship between probability of failure with respect to service life of the fixed offshore platform.

## 5. Conclusions and recommendations

### 5.1. Conclusions

This research has demonstrated a comprehensive assessment of the structural effectiveness of fixed offshore platforms subjected to uniform corrosion. Using Finite Element Analysis in ABAQUS CAE 2022 software and Monte Carlo reliability simulations in PYTHON 3.12 software, we evaluated the degradation of structural integrity under service conditions. The objectives of quantifying the impact of uniform corrosion, assessing intrinsic stress distributions, and predicting reliability over the platform's design life were successfully achieved. Results indicated progressive stress accumulation in critical structural elements, such as beams and column joints, attributed to cross-sectional area depletion. The von Mises, maximum principal, and Tresca stress distributions confirmed that even with acceptable limits for S460 high strength structural steel, continuous corrosion necessitates regular monitoring and maintenance. The reliability analysis further revealed declining reliability indices and increasing probabilities of failure over time, emphasizing the need for proactive structural interventions.

The study also validated that selecting high-grade steel and increasing cross-sectional areas can mitigate stress concentrations and reduce corrosion effects, ensuring extended service life. By aligning computational modeling with design standards such as AASHTO LRFD Bridge Design Specifications and AWS D1.1 Structural Welding Code, this work contributes valuable insights for improving the durability and safety of offshore platforms in challenging marine environments.

### 5.2. Recommendations

The adoption of high-grade steel with superior corrosion resistance and fatigue properties is recommended to slow the degradation process and maintain structural effectiveness over time. Regular inspection and application of corrosion protection measures, such as coatings or cathodic protection, should be incorporated into the platform's lifecycle management.

## References

- Abejide, K., Akadang, O. L. B., & Abejide, O. S. (2022). Stochastic Evaluation of Structural Steel Plates Corrosion in Offshore Platforms. *Haya: The Saudi Journal of Life Sciences*, 7(5), 163-175. <https://doi.org/10.36348/sjls.2022.v07i05.004>
- American Association of State Highway and Transportation Officials. (2020). *LRFD Bridge Design Specifications* (9th Ed.). American Association of State Highway and Transportation Officials.
- American Institute of Steel Construction. (2024). *AISC Student Steel Bridge Competition*. [https://www.aisc.org/globalassets/aisc/university-programs/ssbc/rules/ssbc-2024-rules\\_final.pdf](https://www.aisc.org/globalassets/aisc/university-programs/ssbc/rules/ssbc-2024-rules_final.pdf)
- American Welding Society. (2020). AWS D1.1/D1.1M: Structural Welding Code – Steel (23rd Ed.). American Welding Society. [https://pubs.aws.org/Download\\_PDFS/D1.1-D1.1M-2015-PV.pdf?srsId=AfmBOoo13mUQ0-yYri65tN1UHx\\_4NOSb7RFxHbwmXRcrD55Y7rWgV8LI](https://pubs.aws.org/Download_PDFS/D1.1-D1.1M-2015-PV.pdf?srsId=AfmBOoo13mUQ0-yYri65tN1UHx_4NOSb7RFxHbwmXRcrD55Y7rWgV8LI)
- Brijder, R., Hagen, C. H., Cortés, A., Irizar, A., Thibbotuwa, U. C., Helsen, S., Vásquez, S., & Ompusunggu, A. P. (2022). Review of corrosion monitoring and prognostics in offshore wind turbine structures: Current status and feasible approaches. *Frontiers in Energy Research*, 10, Article 991343. <https://doi.org/10.3389/fenrg.2022.991343>
- Chen, B. Q., Liu, K., & Xu, S. (2024a). Recent advances in aluminum welding for marine structures. *Journal of Marine Science and Engineering*, 12(9), Article 1539. <https://doi.org/10.3390/jmse12091539>
- Chen, M. T., Gong, Z., Cao, H., Zhang, J., Ren, F., Ho, J. C. M., & Lai, M. (2024b). Residual mechanical properties of corroded ultra-high-strength steels and weld metals. *Thin-Walled Structures*, 205, Article 112397. <https://doi.org/10.1016/j.tws.2024.112397>
- Dutta, A., Pal, S. K., & Panda, S. K. (2024). Friction stir seam-and spot-welded aluminium honeycombs: Enhanced structural integrity eliminating adhesive bonding challenges. *Journal of Materials Processing Technology*, 330, Article 118449. <https://doi.org/10.1016/j.jmatprot.2024.118449>
- Elqars, E., Bimoussa, A., Barhoumi, A., Laamari, Y., Byadi, S., Oubella, A., Riadi, Y., Essadki, A., Auhmani, A., & Itto, M. Y. A. (2024). Synthesis and characterization of bis-isoxazoline-thiosemicarbazone as a corrosion inhibitor for carbon steel: Experimental study, and molecular simulation. *Journal of Molecular Structure*, 1312, Article 138476. <https://doi.org/10.1016/j.molstruc.2024.138476>

- European Committee for Standardization. (2023). *Hot rolled products of structural steels - Part 4: Technical delivery conditions for thermomechanical rolled weldable fine grain structural steels* (EN Standard No 10025-4:2023).
- Ghanadi, M., Hultgren, G., Narström, T., Clarin, M., & Barsoum, Z. (2024). Fatigue assessment of welded joints-size effect and probabilistic approach. *Journal of Constructional Steel Research*, 221, Article 108884. <https://doi.org/10.1016/j.jcsr.2024.108884>
- He, Z., He, C., Ma, G., Yang, W., & Kang, X. (2023). Performance assessment of partially corrosion-damaged RC segment incorporating the spatial variability of steel corrosion. *Construction and Building Materials*, 371, Article 130789. <https://doi.org/10.1016/j.conbuildmat.2023.130789>
- Kollár, D. (2023). Numerical modelling on the influence of repair welding during manufacturing on residual stresses and distortions of T-joints. *Results in Engineering*, 20, Article 101535. <https://doi.org/10.1016/j.rineng.2023.101535>
- International Organization for Standardization. (2020a). *Petroleum and natural gas industries – Fixed steel offshore structures* (ISO Standard No. 19902:2020). <https://www.iso.org/standard/65688.html>
- International Organization for Standardization. (2020b). *Petroleum and natural gas industries – Specific requirements for offshore structures. Part 3: Topsides structure* (ISO Standard No. 19901-3:2020). <https://www.iso.org/standard/65041.html>
- Pradhan, R., Joshi, A. P., Sunny, M. R., & Sarkar, A. (2022). Performance of predictive models to determine weld bead shape parameters for shielded gas metal arc welded T-joints. *Marine Structures*, 86, Article 103290. <https://doi.org/10.1016/j.marstruc.2022.103290>
- Rautiainen, M., Remes, H., Niemelä, A., & Romanoff, J. (2023). Fatigue strength assessment of complex welded structures with severe force concentrations along a weld seam. *International Journal of Fatigue*, 167, Article 107321. <https://doi.org/10.1016/j.ijfatigue.2022.107321>
- Saufnay, L., Jaspard, J. P., & Demonceau, J. F. (2024). Improvement of the prediction of the flexural buckling resistance of hot-rolled mild and high-strength steel members. *Engineering Structures*, 315, Article 118460. <https://doi.org/10.1016/j.engstruct.2024.118460>
- Şeker, Ö. (2021). *A practical finite element model of tsadwa type semi-rigid connections for push-over analysis of steel frames in SAP2000* [Master's thesis, Izmir Institute of Technology].
- Walter, N. M. B., Lemos, G. V. B., Kieckow, G. S., Buzzatti, D. T., Buzzatti, J. T., Mattei, F., Reguly, A., Clarke, T., Paes, M. T. P., Dalpiaz, G., & Marinho, R. R. (2024). Investigating microstructure, mechanical properties, and pitting corrosion resistance of UNS S32760 super duplex stainless steel after linear friction welding. *Journal of Materials Research and Technology*, 31, 1637-1643. <https://doi.org/10.1016/j.jmrt.2024.06.191>
- Wang, H., Wang, J., Cao, J., Zhao, J., Qian, W., & Du, H. (2024a). Optimization design of main hinge joint structure based on weld failure analysis. *Engineering Failure Analysis*, 163, Article 108447. <https://doi.org/10.1016/j.engfailanal.2024.108447>
- Wang, L., Qian, X., & Feng, L. (2024b). Effect of welding residual stresses on the fatigue life assessment of welded connections. *International Journal of Fatigue*, 189, Article 108570. <https://doi.org/10.1016/j.ijfatigue.2024.108570>
- Zhou, H., Kinefuchi, M., Takashima, Y., & Shibnuma, K. (2024). Multiscale modelling strategy for predicting fatigue performance of welded joints. *International Journal of Mechanical Sciences*, 284, Article 109751. <https://doi.org/10.1016/j.ijmecsci.2024.109751>

---

## Efektywność Konstrukcyjna Stałych Platform Morskich w Kontekście Równomiernej Korozji

### Streszczenie

W artykule przedstawiono skuteczność strukturalną stałych platform morskich, rozwiązując problemy związane ze złożonymi warunkami obciążenia w środowiskach morskich. Wydajność strukturalną stałej platformy morskiej oceniono przy użyciu analizy metodą elementów skończonych wykonanej w oprogramowaniu ABAQUS CAE, ze szczególnym uwzględnieniem wpływu naprężeń wewnętrznych wywołanych korozją oraz obciążeń środowiskowych, takich jak wiatr, fale i działania operacyjne. Niezawodność stałej platformy morskiej oceniono również przy użyciu metody niezawodności Monte Carlo. W badaniu wykorzystano zaawansowane równania projektowe do oceny niezawodności strukturalnej i szybkości korozji stałej platformy morskiej w celu oszacowania bezpieczeństwa konstrukcji. Wyniki wykazały, że w połączeniach belek i kolumn oraz w kolumnach występują wysokie wartości naprężeń ze względu na efekt zmniejszającego się pola

przekroju poprzecznego w stosunku do czasu, a także naprężeń wewnętrznych w wyniku zastosowanych obciążeń. Stąd wybór stali wysokiej jakości i większego pola przekroju poprzecznego dla elementów konstrukcyjnych spowalnia szybkość korozji, a także zmniejsza naprężenia wewnętrzne konstrukcji spowodowane obciążeniami. Nie tylko poprawia to nośność, ale także znacznie zmniejsza ryzyko awarii konstrukcyjnej, co dobrze wpisuje się w dane doświadczalne. Ponadto badanie podkreśliło znaczenie uwzględnienia interakcji między właściwościami materiału, cechami połączenia i warunkami obciążenia w procesie projektowania. Wyniki te przyczynią się do rozwoju bardziej wytrzymałych i trwałych stałych platform morskich, zapewniając ich bezpieczeństwo i długowieczność w wymagających środowiskach operacyjnych.

**Słowa kluczowe:** korozja, analiza elementów skończonych, stałe platformy morskie, spoina

---